ARTICLE

Cell Behaviors on Polysaccharide-Wrapped Single-Wall Carbon Nanotubes: A Quantitative Study of the Surface Properties of Biomimetic Nanofibrous Scaffolds

Xiaoke Zhang,[†] Lingjie Meng,[†] and Qinghua Lu[†,‡,*]

[†]School of Chemistry and Chemical Technology and [‡]State Key Laboratory of Metal Matrix Composites, Shanghai Jiao Tong University, Shanghai 200240, People's Republic of China

ABSTRACT Natural polysaccharides such as amylose (AMY), alginate sodium (ALG), and chitosan (CHI) have been noncovalently wrapped onto single-wall carbon nanotubes (SWCNTs) to give a series of SWCNT scaffolds, termed as AMY-SWCNT, ALG-SWCNT, CHI-SWCNT, and CHI/ALG-SWCNT scaffolds. Compared to purified SWCNTs and oxidized SWCNTs, the polysaccharide-wrapped SWCNTs can well mimic nanofibrous extracellular matrix and significantly enhance cell adhesion and proliferation. The surface properties of the SWCNT scaffolds, such as functional groups, surface charge, and hydrophilicity, can all directly influence the protein adsorption and lead to changes in cellular FAK expression, thus affect the mammalian cell morphology and proliferation. By quantitatively studying the surface properties of these SWCNT scaffolds, it can be concluded that relatively positively charged hydrophilic scaffolds that bear —OH groups can remarkably promote cell growth. Considering all properties, the relatively electrical neutral and hydrophilic AMY-SWCNT scaffolds bearing only —OH groups are able to sustain the highest cell viability after 72 h culturing.

KEYWORDS: single-wall carbon nanotubes · polysaccharide · scaffold · surface properties

A major goal of tissue engineering is to produce artificial biological substitutes that have the capacity to sustain and direct cell adhesion, growth, and proliferation and thus to restore or repair the damaged or diseased tissues.[1] An ideal scaffold should mimic both the structural and biological functions of native extracellular matrix (ECM) to provide mechanical support and regulate cell activities.[2] Generally, cells adhere and grow on the ECM consisting of collagen multifibrils (50−500 nm of diameter) and proteoglycans in native tissue. However, the direct utility of collagen and proteoglycans has been limited due to their high price and fragile mechanical properties. The high strength fiber-reinforced natural biopolymers are architecturally similar to the collagen structure of the ECM and thus can be considered as alternative substitutes.[3] Cell adhesion to biomaterial surface has to be mediated by a layer of adsorbed ECM proteins such as immunoglobulins, vitronectin, fibrinogen, and fibronectin,[4,5] which can enhance cellular adhesion onto artificial biomaterials and help to speed up the tissue regeneration. The surface characteristics of biomaterials, such as surface charge, surface functional groups, hydrophilicity, and topography, may affect the type, quantity, conformation, or activity of the absorbed proteins and thus influence the cell adhesion, migration, and proliferation.[6−10]

Carbon nanotubes (CNTs) are a man-made form of carbon that did not exist until the 1990s. They have one-dimensional nanoscale structure, excellent flexibility, and electrical conductivity, high strength, and stiffness. These outstanding properties make them ideal reinforcement materials to improve the mechanical properties of biomaterials for tissue engineering.[11−13] The biomolecule can be covalently attached onto the nanotube surface[14−16] or can noncovalently encase nanotubes,[17−28] with the latter showing obvious advantages because it requires relatively mild reaction conditions and the perfect graphitic structure of CNTs can be maintained. Over the past decades, many natural biomaterials such as polysaccharides,[17−22] DNA,[23,24] proteins,[25] polypeptides,[26−28] and synthetic polymers such as poly(phenylacetylene)[29−31] have been reported to wrap around CNTs *via* noncovalent interactions. Especially, the polysaccharides are much more attractive because they are cheap and readily available. Differ-

*Address correspondence to qhlu@sjtu.edu.cn.

Received for review June 17, 2009 and accepted August 26, 2009.

Published online August 31, 2009. 10.1021/nn9006362 CCC: $40.75

ent types of polysaccharides have been applied to modify CNTs, which would be able to endow different surface properties for the CNT composites. Although factors that affect the cell behaviors have begun to be understood,[14−16] quantitative investigations on the relationship between the surface properties and the cell behaviors remain yet to be explored.

In this study, we used three types of natural polysaccharides, amylose (AMY), alginate sodium (ALG), and chitosan (CHI), to noncovalently wrap the single-wall carbon nanotubes (SWCNTs) to construct four types of SWCNT scaffolds, termed as AMY-SWCNT, ALG-SWCNT, CHI-SWCNT, and CHI/ALG-SWCNT scaffolds. High-resolution transmission electron microscopy (HR-TEM) and atomic force microscope (AFM) were used for the characterization of the obtained modified SWCNTs. By investigating the interactions between the SWCNT scaffolds and mammalian cells, we found that all of the poly-saccharide-wrapped SWCNTs could enhance the cell viability compared to purified SWCNT and oxidized SWCNT scaffolds, and thus special efforts have been focused on characterization of these polysaccharide−SWCNT complexes in a more quantitative way. For this reason, we investigated the surface functional groups, ζ potentials (surface charge), and water contact angles (hydrophilicity) of the resulted SWCNTs. Compared to the surface with $-COO^-$ or $-NH_2$ groups, low ζ potential, and high contact angles, it was found that the surface with only −OH groups, higher ζ potential, and lower contact angles are beneficial to the cell growth. Among all of the SWCNT scaffolds prepared in this study, the electrical neutral and hydrophilic AMY-SWCNT scaffolds bearing only −OH groups can sustain the highest cell viability.

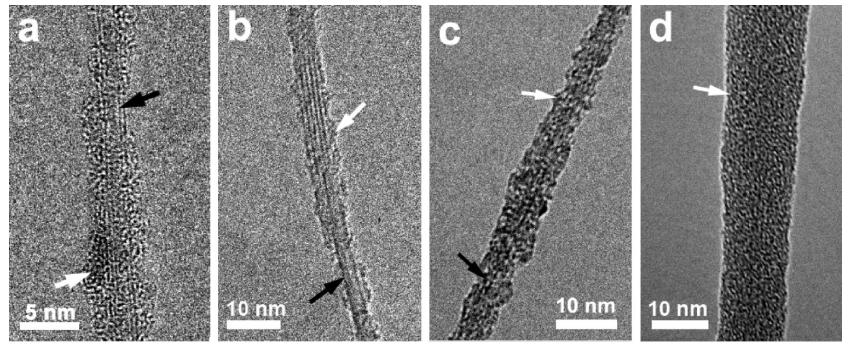

Figure 1. TEM images of (a) AMY-SWCNTs, (b) ALG-SWCNTs, (c) CHI-SWCNTs, and (d) CHI/ALG-SWCNTs.

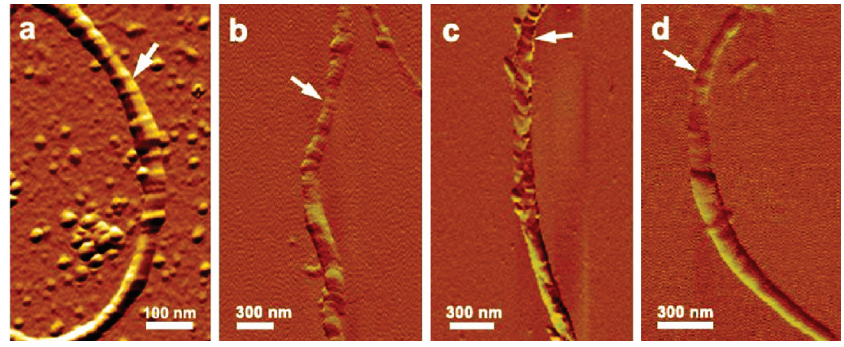

Figure 2. AFM images show the helical structures on (a) AMY-SWCNTs, (b) ALG-SWCNTs, (c) CHI-SWCNTs, and (d) CHI/ALG-SWCNTs.

RESULTS AND DISCUSSION

The impurities in commercial SWCNTs, such as metal catalysts and amorphous carbon particles, are reported to be toxic to cells and could induce intracellular reactive oxygen species (ROS).[34,35] Thus, all of the SWCNTs in this study are purified using a literature method.[32] It is known that SWCNTs tend to form bundles due to their high aspect ratios and the strong intertube van der Waals interactions, thus their dispersion in common solvents is very limited. Natural polysaccharides could be used to noncovalently wrap around SWCNTs, imparting water solubility of the nanotubes.[18,20,21] Figure 1a−c shows the structure of AMY-SWCNTs, ALG-SWCNTs, and CHI-SWCNTs, respectively. The loosely wrapped polysaccharide chains (white arrows) can be observed on the side walls (black arrows) of a single SWCNT or a SWCNT bundle. With addition of ALG-SWCNTs into a CHI solution, both ALG and CHI can "doubly" wrap onto SWCNTs. The double-layered polysaccharide-wrapped SWCNTs (CHI/ALG-SWCNTs) show additional thickness (Figure 1d), but the side walls could not be observed due to the thick bilayer of CHI/ALG around the SWCNTs.

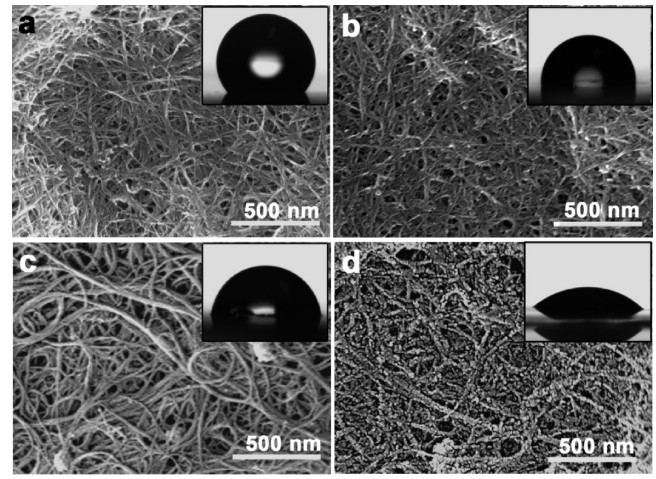

Figure 3. SEM images of various types of SWCNT scaffolds. (a) Purifed SWCNTs, (b) oxidized SWCNTs, (c) AMY-SWCNTs, and (d) CHI/ALG-SWCNTs. Inset: images of water drops on the surfaces of SWCNT scaffolds.

TABLE 1. Zeta Potentials of Modified Nanotubes and Wettability of the Resulting SWCNT Scaffolds

	contact angle (°)[a]	ζ potential (mV)[a]
purified SWCNTs	120 ± 4	−36.13 ± 2.05
oxidized SWCNTs	97 ± 4	−55.90 ± 2.42
AMY-SWCNTs	81 ± 3	−11.19 ± 1.62
ALG-SWCNTs	95 ± 3	−41.13 ± 0.38
CHI-SWCNTs	99 ± 3	+6.22 ± 0.22
CHI/ALG-SWCNTs	41 ± 6	−26.10 ± 0.3

[a]All of the data were averaged from three measurements.

AFM was also employed for characterization of the polysaccharide-modified SWCNTs, and helical morphology is found in the AMY-SWCNTs (Figure 2a), ALG-SWCNTs (Figure 2b), CHI-SWCNTs (Figure 2c), and CHI/ALG-SWCNT samples (Figure 2d), which is in accordance with previous reports that polysaccharides tend to wrap around SWCNTs in a helical manner.[19,21,22]

By vacuum filtration, the SWCNTs can be well-fixed on the porous PVDC membranes. SEM images (Figure 3) showed that the scaffolds were all well-covered with modified SWCNTs, and all types of SWCNT scaffolds show nanofibrous structure in our experiment (images of ALG-SWCNT and CHI-SWCNT scaffolds are quite similar with Figure 3c and are not given). The purified SWCNTs can be considered as a single sheet of graphite rolled into a cylindrical shape with only a few $-COO^-$ and $-OH$ groups at their surface defects. The purified SWCNTs have hydrophobic and negatively charged surface with 120° contact angle and about −36.13 mV ζ potential (see Figure 3a and Table 1). Oxidation would introduce more $-COO^-$ groups on their surface, thus oxidized SWCNTs have more negatively charged surface (∼−55.90 mV ζ potential) and improved hydrophilicity with a contact angle of *ca.* 97°. Similarly, ALG, CHI, and AMY would introduce different functional groups such as $-COO^-$, $-OH$, and $-NH_2$ onto SWCNTs after wrapping around them. On one hand, these polar and highly hydrophilic functional groups could increase the surface energy and make the surfaces of the SWCNT scaffolds more hydrophilic (see Figure 3c,d and Table 1). For example, The CHI/ALG-SWCNT scaffold has the most hydrophilic surface with the lowest contact angle, which might be due to the fact that the "bilayer" of CHI/ALG has increased number of hydrophilic functional groups on the surface. On the other hand, these polysaccharides also have different surface charge and could change the ζ potential of the SWCNTs (see Table 1). For instance, CHI-SWCNTs have the highest ζ potential with the coating of positively charged CHI. In contrast, after wrapping by negatively charged ALG, the resulted ALG-SWCNTs have the lowest ζ potential in all of these polysaccharide−SWCNT composites. Also, the ζ potential of polysaccharide−SWCNTs should be fine-tuned by varying the ALG/CHI ratios. These SWCNT scaffolds provide us a chance to quantitatively investigate the relationship of the surface properties of the CNT scaffolds (surface functional groups, surface charge, and hydrophilicity, *etc.*) with the cell behaviors, which can guide us to develop optimal CNT scaffolds for cell growth.

First of all, AO/EB double staining was used to study the growth and development traits of HeLa cells on all types of SWCNT scaffolds. Healthy cells have green nuclei, uniform chromatin, and intact cell membrane on the glass slide (Figure 4a), while the cells in necrosis or in a late stage of apoptosis have red nuclei with damaged cell membrane.[33] After culturing for 72 h, some of the cells cultured on the purified SWCNT scaffold were in necrosis with red nuclei (Figure 4b), while relatively less necrotic cells were found on oxidized SWCNT scaffolds or polysaccharide-wrapped SWCNT scaffolds (Figure 4e−g), indicating that HeLa cells can grow on all of the SWCNT scaffolds and the modified SWCNT scaffolds have improved biocompatibility.

WST-1 assay was further carried out to quantitatively compare the biocompatibility of these SWCNT scaffolds by detecting the viability of HeLa cell growth on them. After culturing for 72 h, the majority of cells had undergone proliferation. Compared to the control sample, a significant loss in cell viability was observed for the purified SWCNT scaffold with the cell viability of 61.8 ± 5.4% (Figure 5a). After oxidization or polysaccharide wrapping, hydrophilic

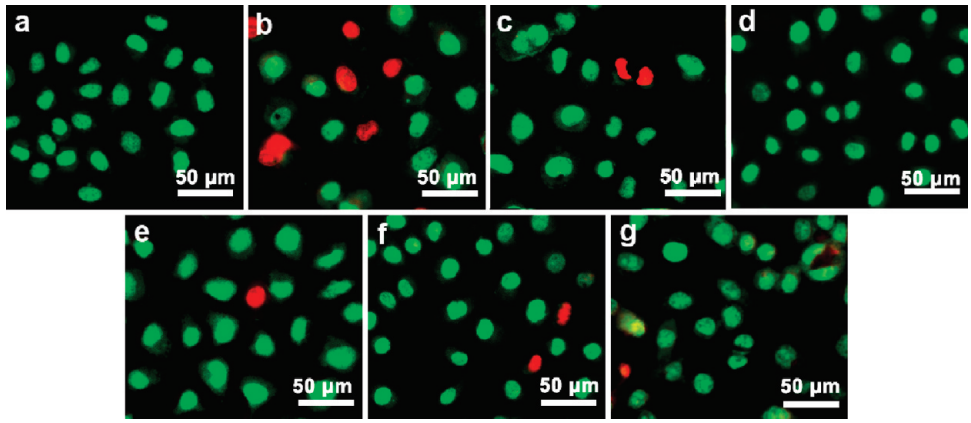

Figure 4. Fluorescence microscopy images of HeLa cells cultured on (a) a glass slide, (b) purified SWCNTs, (c) oxidized SWCNTs, (d) AMY-SWCNTs, (e) CHI-SWCNTs, (f) ALG-SWCNTs, and (g) CHI/ALG-SWCNT scaffolds for 72 h. The cells were stained by AO and EB.

groups such as $-COO^-$, $-OH$, and $-NH_2$ were introduced onto the surface of SWCNT scaffolds. The cell viability on these modified SWCNT scaffolds was thus increased at different degrees (Figure 5a). It is also shown in Figure 5a that AMY-SWCNT scaffold with only $-OH$ groups could sustain the highest cell viability (148.6 ± 6.2%) after 72 h culturing. The $-NH_2$ and $-COO^-$ groups are relatively the least capable of promoting the growth of HeLa cells. The result is in accordance with the previous report[8] that suggests that functional groups including $-OH$, $-NH_2$, and $-COOH$ may modulate the structure and molecular composition of cell-matrix adhesions, and the substrate with $-OH$ groups shows the highest effective cell adhesion strength. However, the exact mechanism is not clear, and further studies are still in process in our laboratory.

It is already known that the surface functional groups are not the only factors affecting the cell adhesion; other surface properties such as surface charge and hydrophilicity should be considered at the same time.[6−10] The cell viability on the SWCNT scaffolds increased in the following order: purified SWCNTs < oxidized SWCNTs < ALG-SWCNTs < CHI/ALG-SWCNTs < CHI-SWCNTs < AMY-SWCNTs, which is partly related to the ascending order of modified SWCNT ζ potentials and the descending order of water contact angles (Figure 5b,c). Generally, cellular membranes are negatively charged, and thus cells can more easily attach and grow on more positively charged surfaces. Therefore, the cell viability on ALG-SWCNT, CHI/ALG-SWCNT, and CHI-SWCNT scaffolds increased with the ascending of their ζ potentials. Figure 5c gives the water contact angles and the cell viability on the purified SWCNTs, oxidized SWCNTs, ALG-SWCNTs, AMY-SWCNTs, and CHI/ALG-SWCNTs. It can be concluded that the cell viability on these SWCNT scaffolds almost increased with the ascending of their hydrophilicity, which showed us that cells prefer to grow and proliferate on a hydrophilic surface.

It should be noted that the abnormal point in Figure 5b,c is the cell viability on the AMY-SWCNTs. In Figure 5b, the slightly negatively charged AMY-SWCNTs (~−11.19 mV ζ potential) have higher cell viability than the positively charged CHI-SWCNTs (~+6.22 mV ζ potential) probably due to the more hydrophilic surface and the only favorite functional groups of $-OH$. Similarly, though CHI/ALG-SWCNTs have the most hydrophilic surface in Figure 5c, AMY-SWCNTs still sustain the higher cell viability because of their relatively positively charged surface and owning the only favorite functional groups of $-OH$. These results further demonstrated that surface functional groups, surface charge, and the hydrophilicity all play key roles in cell growth. These rules can guide us to develop optimal CNT scaffolds for cell growth.

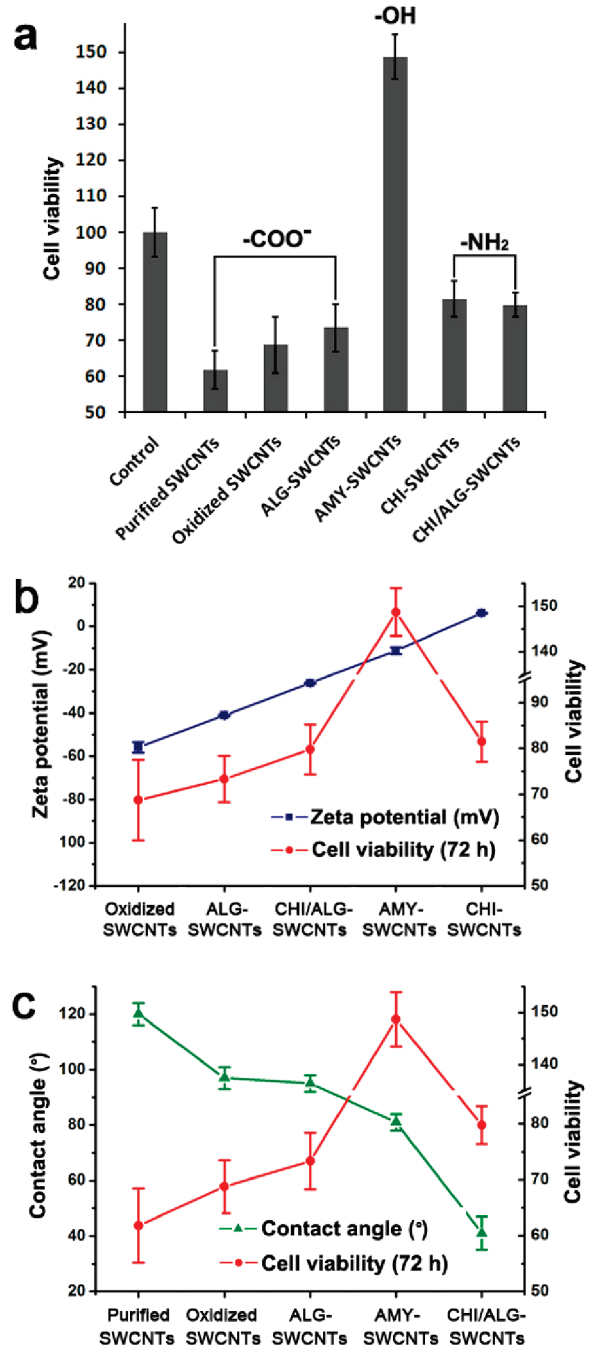

Figure 5. Influence of surface properties on cell viability. (a) Influence of functional groups on cell viabilities. (b) Influence of surface charge of SWCNTs on cell viability. (c) Influence of surface hydrophilicity/hydrophobicity on cell viability. HeLa cells were growth on various types of SWCNT scaffolds and cultured for 72 h. Cells cultured on a glass slide were used as control.

In order to further study the differences of cell viability on different scaffolds, we have also investigated the cell adhesion and morphology on a glass slide and SWCNT scaffolds by using SEM. It can be observed from Figure 6a and its magnified picture around the black arrow (Figure 6e) that a HeLa cell is well spread and attaches closely to the glass slide

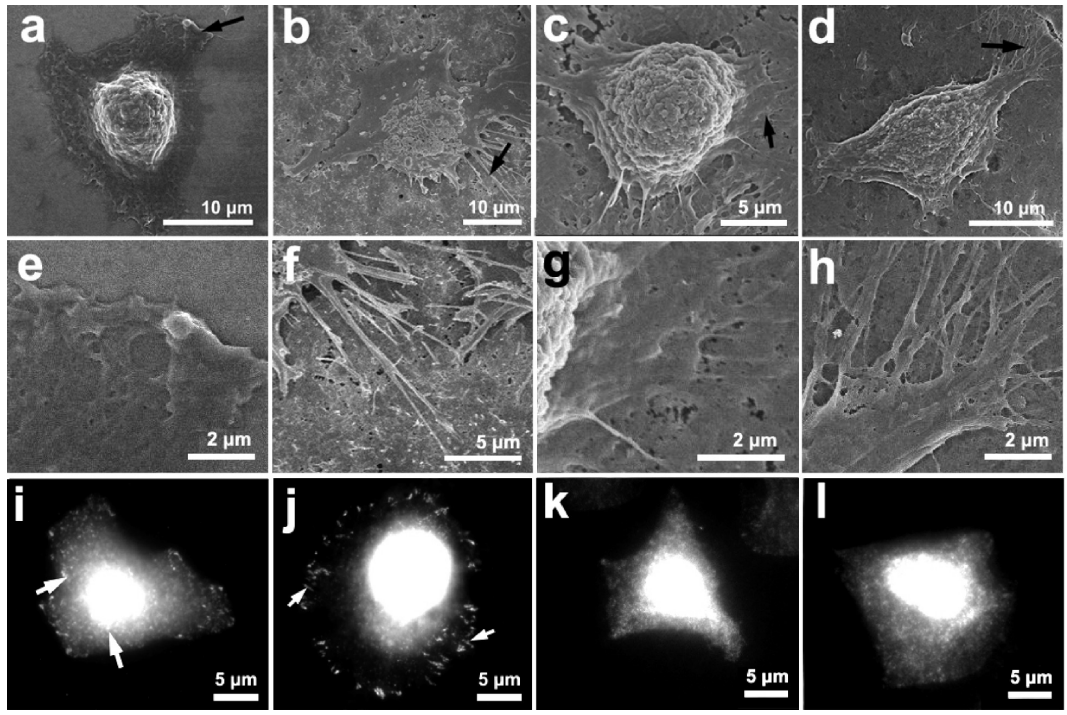

Figure 6. SEM images of HeLa cells cultured on (a,e) glass slide, (b,f) purified SWCNTs, (c,g) CHI-SWCNTs, and (d,h) AMY-SWCNT scaffolds. Fluorescence images of FAK distribution in HeLa cells cultured on (i) glass slide, (j) purified SWCNTs, (k) CHI-SWCNTs, and (l) AMY-SWCNT scaffolds. All of the cells were cultured for 12 h.

with lamellipodia seen at the periphery. On the hydrophobic purified SWCNT scaffold, the cell body shows an incompletely spread morphology (Figure 6b) with less lamellipodia but some elongated and radial filopodia seen at the periphery (Figure 6b,f), showing poor adhesion. Compared to the cell on the purified SWCNTs, it could be seen that the cells show good attachment with less or no projection of elongated filopodia and more lamellipodia on CHI-SWCNTs (Figure 6c) and AMY-SWCNTs (Figure 6d). However, the cell on the CHI-SWCNT scaffold shows a less spread spherical shape with a few elongated filopodia (Figure 6c,g), while the cell on the AMY-SWCNT scaffold appears well-spread with extensive network of cell lamellopodia and filopodia (Figure 6h) attached to the scaffold, suggesting the AMY-SWCNT scaffolds have the best surface properties for the cell adhesion, which can partly explain the highest cell viability on them.

It is known that cell adhesion to ECM is usually mediated by focal adhesions (FAs), which link actin cytoskeleton to ECM and provide regions for signal transduction to regulate cell growth.[36] The focal adhesion kinase (FAK) is a protein tyrosine kinase which is recruited at an early stage to FAs and is implicated in signaling pathways and regulates cell cytoskeletal organization, adhesion, migration, survival, and proliferation.[37−40] Here, FAK was chosen to be immunostained and observed by fluorescence microscopy to investigate the focal adhesion formation on different scaffolds (Figure 6i−l). It could be observed that the FAKs were distributed with a few aggregates in the entire ventral cell surface in the control group (Figure 6f). When cells cultured on purified SWCNTs, FAK aggregates were annularly distributed at the periphery of cells (Figure 6j), indicating a rather weak cell adhesion.[41] Interestingly, the cells cultured on polysaccharide-modified SWCNTs show no obvious FAK aggregates. Instead, relatively homogeneous distribution in the whole cell body (Figure 6k,l) was observed, suggesting a much stronger adhesion. On the basis of the above results, it can be concluded that the surface properties of scaffolds could affect the cell adhesion and FAK distribution, thus leading to changes in the cell morphology and viability. AMY-SWCNTs can be regarded as excellent substitutes to mimic native ECM, which can well-sustain and direct cell adhesion, growth, and proliferation.

CONCLUSIONS

In conclusion, natural polysaccharides such as amylose (AMY), alginate sodium (ALG), and chitosan (CHI) were noncovalently wrapped onto single-wall carbon nanotubes (SWCNTs). The relationship of the surface properties with the cell behaviors has been investigated in a more quantitative way. Compared to purified SWCNTs and oxidized SWCNTs, the polysaccharide-wrapped SWCNTs could enhance cell adhesion and proliferation significantly. We found surface properties of scaffolds could directly influence the protein adsorption leading to different cellular FAK expression, thus affecting the cell morphology, migration, and proliferation. Notably, compared to the hydrophobic, negatively

charged surfaces with $-COO^-$ and $-NH_2$ groups, the hydrophilic, positively charged surfaces with only $-OH$ groups are beneficial to cell growth. Integrating these factors, electrically neutral and hydrophilic AMY-SWCNT scaffolds bearing only $-OH$ groups can sustain the highest cell viability.

METHODS

Materials. Commercial SWCNTs (purity > 90%; length > 50 μm; diameter = 1−2 nm) were purchased from Chengdu Organic Chemistry Co., Ltd. AMY was purchased from National Starch & Chemical Company. ALG was purchased from Acros. CHI was obtained from TCI (Tokyo). Acridine orange (AO), ethidium bromide (EB), and Triton X-100 were all obtained from Sigma-Aldrich. Fetal bovine serum (FBS) and high glucose Dulbecco's Modified Eagle's medium (DMEM) were obtained from Hyclone. WST-1 reagent was purchased from Beyondtime Bio-Tech. Mouse IgG1 antifocal adhesion kinase (FAK) was purchased from BD Biosciences. Rhodamine-conjugated goat antimouse IgG was obtained from KangChen Bio-Tech. Porous poly(vinylidene chloride) (PVDC) membrane was purchased from Shanghai ANPEL Instrument Co. Ltd. (0.45 μm pore size). Other reagents were obtained from Shanghai Chemical Reagents Corporation. Human cervical carcinoma HeLa cells were cultured in high glucose DMEM supplemented with 10% FBS in a humidified incubator (MCO-15AC, Sanyo) at 37 °C in which the CO_2 level was kept constant at 5%.

Measurements. High-resolution transmission electron microscopy (HR-TEM) was conducted on a JEOL TEM-2100. Atomic force microscopy (AFM) was performed on a Vecco AFM NanoScope III. Zeta potentials of all the nanotubes were measured by a ζ potential analyzer (Zetasizer Nano ZS90, Malvern). Scanning electron microscopy was conducted on a JEOL JSM-7401F. The room-temperature static contact angle of water on the SWCNT scaffolds was determined with a goniometer (OCA-20, Dataphysics) by the sessile drop method. The fluorescent photos were obtained by using an inverted fluorescence microscope (IX 71, Olympus) with a charge-coupled device (CCD, Cascade 650).

Purification and Oxidation of SWCNTs. The purchased SWCNTs (1.0 g) were refluxing in HNO_3 aqueous solution (2.6 mol/L, 200 mL) under magnetic stirring for 24 h for purification.[32] The purified SWCNTs were filtered through a PVDC membrane and washed several times with ultrapure water to neutrality. The product was then dried under vacuum at 50 °C for 24 h for further use. Purified SWCNTs (100 mg) were dispersed in a mixture of 98% H_2SO_4 and 65% HNO_3 (3:1 v/v, 100 mL) and exposed to sonic irradiation at 0 °C for 6 h to prepare the oxidized SWCNTs. After washing with ultrapure water (18.2 MΩ), the sample was collected and dried under vacuum at 50 °C for 24 h.

Preparation of Polysaccharide-Wrapped SWCNTs. AMY-SWCNTs were prepared according to our previous procedures.[22] Purified SWCNTs (2.5 mg) were dispersed in ultrapure water (85 mL) and presonicated for 1 h, and then amylose−DMSO solution (16.7 mg/mL, 15 mL) was added dropwise into the sonicating suspension. The mixture was sonicated for another 10 min and kept at room temperature for 24 h. After centrifuging for 30 min, the sediment was dispersed in ultrapure water with sonication and centrifugation again, which was repeated at least eight times. ALG solution (1 mg/mL) and CHI solution (1 mg/mL in 0.02 M acetic acid) were used to prepare ALG-SWCNTs, CHI-SWCNTs, and CHI/ALG-SWCNTs. Purified SWCNTs (20 mg) were sonicated in 40 mL of polysaccharide solution for 20 min and then stirred overnight at room temperature to obtain ALG-SWCNTs or CHI-SWCNTs. The obtained ALG-SWCNTs (10 mg) were again sonicated for 20 min in 20 mL of CHI solution and stirred overnight at room temperature to obtain the CHI/ALG-SWCNT complex. All of the ALG- or CHI-modified SWCNT samples were collected by filtration through PVDC membrane and washed with ultrapure water to remove excess of polysaccharides, then collected and dried at room temperature.

Preparation of the SWCNT Scaffolds. The SWCNT scaffolds were all made by vacuum filtration of the modified SWCNT aqueous dispersions onto porous PVDC membranes and then dried at 60 °C for 3 h, thus SWCNTs were coated and fixed on membranes. All of the SWCNT scaffolds were sterilized under ultraviolet light overnight before further use.

Fluorescence Microscopy. DNA-binding dyes AO and EB were further used for the morphological detection of apoptotic and necrotic cells.[33] After being cultured on SWCNT scaffolds or on a glass slide for 72 h, HeLa cells were washed by sterilized PBS and stained with a mixture of AO (5 μg/mL) and EB (5 μg/mL) at room temperature for 5 min. The stained cells were observed by an inverted fluorescence microscope, and images were taken by a CCD camera.

Cell Viability Test. WST-1 assay was used to measure cell viability.[34] SWCNT scaffolds were placed into a 24-well flat culture plate (Corning), and then a HeLa cell suspension (500 μL) was transferred to each well. The cells were cultured for 72 h. Sterilized phosphate buffered salt solution (PBS, 0.01 M, pH 7.4, 500 μL) was used to substitute the culture medium, before adding 1/10 (v/v) of WST-1 reagent. The cells were incubated for another 2 h. Then the suspension in each well (100 μL) was transferred to a 96-well flat plate (Corning), and the absorbance was measured at 450 nm using a microplate reader (Model 680, Bio-Rad). The cells cultured on glass slides at the same time intervals were used as controls (100% of viability), and background absorbance was measured in the culture medium without cells and CNTs.

SEM Analysis and Immunocytochemical Staining. SEM was used to investigate the cell morphology on SWCNT scaffolds. After culturing on SWCNT scaffolds for 12 h, HeLa cells were fixed with 2.5% glutaraldehyde for 1.5 h at 4 °C, postfixed in 1% OsO_4 for 2 h, and dehydrated using a graded ethanol series. Critical point-dried samples were sputtered with gold before investigating by SEM. For immunocytochemical staining, after culturing on SWCNT scaffolds for 12 h, HeLa cells were fixed with 3.7% formaldehyde in PBS at room temperature for 10 min and washed with PBS three times. Then the cells were permeated with 0.1% Triton X-100 at room temperature for 5 min and washed with PBS three times. After incubating with blocking buffer (3% FBS in PBS) at room temperature for 30 min, primary antibody mouse IgG1 anti-FAK (1:200, v/v) was added and incubated at 4 °C overnight. The cells were washed with PBS three times. Rhodamine-conjugated goat antimouse IgG (1:200, v/v) was added and incubated at room temperature for 30 min. An inverted fluorescence microscope was used to observe the samples, and images were taken by a CCD camera.

Acknowledgment. We gratefully acknowledge the financial support from the National Science Fund for Distinguished Young Scholars and the National Science Foundation of China (20874059), Major Project of Chinese National Programs for Fundamental Research and Development (973 Project: 2009CB930400), the High Technology Research and Development Program of China (863 Project: 2009AA03Z329), Key Fundamental Research Project of Science and Technology Commission of Shanghai Municipal Government (08JC1412300), and Shanghai Leading Academic Discipline Project (No. B202).

REFERENCES AND NOTES

1. Langer, R.; Vacanti, J. P. Tissue Engineering. *Science* **1993**, *260*, 920–926.
2. Park, K. E.; Kang, H. K.; Lee, S. J.; Min, B.-M.; Park, W. H. Biomimetic Nanofibrous Scaffolds: Preparation and Characterization of PGA/Chitin Blend Nanofibers. *Biomacromolecules* **2006**, *7*, 635–643.
3. Malafaya, P. B.; Silva, G. A.; Reis, R. L. Natural-Origin Polymers as Carriers and Scaffolds for Biomolecules and Cell Delivery in Tissue Engineering Applications. *Adv. Drug Delivery Rev.* **2007**, *59*, 207–233.
4. Brash, J. Protein Adsorption at the Solid−Solution Interface in Relation to Blood-Material Interactions. *Proteins at Interfaces*; American Chemical Society: Washington, DC, 1987; pp 490−506.

5. Grinnell, F.; Feld, M.; Minter, D. Fibroblast Adhesion to Fibrinogen and Fibrin Substrata: Requirement for Cold-Insoluble Globulin (Plasma Fibronectin). *Cell* **1980**, *19*, 517–525.
6. Cole, M. A.; Voelcker, N. H.; Thissen, H.; Griesser, H. J. Stimuli-Responsive Interfaces and Systems for the Control of Protein−Surface and Cell−Surface Interactions. *Biomaterials* **2009**, *30*, 1827–1850.
7. Mendonca, G.; Mendonca, D. B. S.; Aragao, F. J. L.; Cooper, L. F. Advancing Dental Implant Surface Technology—From Micron- to Nanotopography. *Biomaterials* **2008**, *29*, 3822–3835.
8. Keselowsky, B. G.; Collard, D. M.; Garcia, A. J. Surface Chemistry Modulates Focal Adhesion Composition and Signaling through Changes in Integrin Binding. *Biomaterials* **2004**, *25*, 5947–5954.
9. Sherratt, M. J.; Bax, D. V.; Chaudhry, S. S.; Hodson, N.; Lu, J. R.; Saravanapavan, P.; Kielty, C. M. Substrate Chemistry Influences the Morphology and Biological Function of Adsorbed Extracellular Matrix Assemblies. *Biomaterials* **2005**, *26*, 7192–7206.
10. Bauer, S.; Park, J.; von der Mark, K.; Schmuki, P. Improved Attachment of Mesenchymal Stem Cells on Super-Hydrophobic TiO_2 Nanotubes. *Acta Biomater.* **2008**, *4*, 1576–1582.
11. Balani, K.; Anderson, R.; Laha, T.; Andara, M.; Tercero, J.; Crumpler, E.; Agarwal, A. Plasma-Sprayed Carbon Nanotube Reinforced Hydroxyapatite Coatings and Their Interaction with Human Osteoblasts *In Vitro*. *Biomaterials* **2007**, *28*, 618–624.
12. Chlopek, J.; Czajkowska, B.; Szaraniec, B.; Frackowiak, E.; Szostak, K.; Beguin, F. *In Vitro* Studies of Carbon Nanotubes Biocompatibility. *Carbon* **2006**, *44*, 1106–1111.
13. Webster, T. J.; Waid, M. C.; McKenzie, J. L.; Price, R. L.; Ejiofor, J. U. Nano-Biotechnology: Carbon Nanofibres as Improved Neural and Orthopaedic Implants. *Nanotechnology* **2004**, *15*, 48–54.
14. Hu, H.; Ni, Y. C.; Montana, V.; Haddon, R. C.; Parpura, V. Chemically Functionalized Carbon Nanotubes as Substrates for Neuronal Growth. *Nano Lett.* **2004**, *4*, 507–511.
15. Mwenifumbo, S.; Shaffer, M. S.; Stevens, M. M. Exploring Cellular Behaviour with Multi-Walled Carbon Nanotube Constructs. *J. Mater. Chem.* **2007**, *17*, 1894–1902.
16. Zanello, L. P.; Zhao, B.; Hu, H.; Haddon, R. C. Bone Cell Proliferation on Carbon Nanotubes. *Nano Lett.* **2006**, *6*, 562–567.
17. Star, A.; Steuerman, D. W.; Heath, J. R.; Stoddart, J. F. Starched Carbon Nanotubes. *Angew. Chem., Int. Ed.* **2002**, *41*, 2508–2512.
18. Kim, O.-K.; Je, J.; Baldwin, J. W.; Kooi, S.; Pehrsson, P. E.; Buckley, L. J. Solubilization of Single-Wall Carbon Nanotubes by Supramolecular Encapsulation of Helical Amylose. *J. Am. Chem. Soc.* **2003**, *125*, 4426–4427.
19. Bae, A. H.; Lee, S. W.; Ikeda, M.; Sano, M.; Shinkai, S.; Sakurai, K. Rod-like Architecture and Helicity of the Poly(C)/Schizophyllan Complex Observed by AFM and SEM. *Carbohydr. Res.* **2004**, *339*, 251–258.
20. Hasegawa, T.; Fujisawa, T.; Numata, M.; Umeda, M.; Matsumoto, T.; Kimura, T.; Okumura, S.; Sakurai, K.; Shinkai, S. Single-Walled Carbon Nanotubes Acquire a Specific Lectin-Affinity through Supramolecular Wrapping with Lactose-Appended Schizophyllan. *Chem. Commun.* **2004**, 2150–2151.
21. Numata, M.; Asai, M.; Kaneko, K.; Bae, A. H.; Hasegawa, T.; Sakurai, K.; Shinkai, S. Inclusion of Cut and As-Grown Single-Walled Carbon Nanotubes in the Helical Superstructure of Schizophyllan and Curdlan (ss-1,3-glucans). *J. Am. Chem. Soc.* **2005**, *127*, 5875–5884.
22. Fu, C.; Meng, L.; Lu, Q.; Zhang, X.; Gao, C. Large-Scale Production of Homogeneous Helical Amylose/SWNTs Complexes with Good Biocompatibility. *Macromol. Rapid Commun.* **2007**, *28*, 2180–2184.
23. Zheng, M.; Jagota, A.; Strano, M. S.; Santos, A. P.; Barone, P.; Chou, S. G.; Diner, B. A.; Dresselhaus, M. S.; McLean, R. S.; Onoa, G. B.; et al. Structure-Based Carbon Nanotube Sorting by Sequence-Dependent DNA Assembly. *Science* **2003**, *302*, 1545–1548.
24. Gigliotti, B.; Sakizzie, B.; Bethune, D. S.; Shelby, R. M.; Cha, J. N. Sequence-Independent Helical Wrapping of Single-Walled Carbon Nanotubes by Long Genomic DNA. *Nano Lett* **2006**, *6*, 159–164.
25. Karajanagi, S. S.; Yang, H.; Asuri, P.; Sellitto, E.; Dordick, J. S.; Kane, R. S. Protein-Assisted Solubilization of Single-Walled Carbon Nanotubes. *Langmuir* **2006**, *22*, 1392–1395.
26. Dieckmann, G. R.; Dalton, A. B.; Johnson, P. A.; Razal, J.; Chen, J.; Giordano, G. M.; Munoz, E.; Musselman, I. H.; Baughman, R. H.; Draper, R. K. Controlled Assembly of Carbon Nanotubes by Designed Amphiphilic Peptide Helices. *J. Am. Chem. Soc.* **2003**, *125*, 1770–1777.
27. Dalton, A. B.; Ortiz-Acevedo, A.; Zorbas, V.; Brunner, E.; Sampson, W. M.; Collins, L.; Razal, J. M.; Yoshida, M. M.; Baughman, R. H.; Draper, R. K.; et al. Hierarchical Self-Assembly of Peptide-Coated Carbon Nanotubes. *Adv. Funct. Mater.* **2004**, *14*, 1147–1151.
28. Zorbas, V.; Ortiz-Acevedo, A.; Dalton, A. B.; Yoshida, M. M.; Dieckmann, G. R.; Draper, R. K.; Baughman, R. H.; Jose-Yacaman, M.; Musselman, I. H. Preparation and Characterization of Individual Peptide-Wrapped Single-Walled Carbon Nanotubes. *J. Am. Chem. Soc.* **2004**, *126*, 7222–7227.
29. Tang, B. Z.; Xu, H. Y. Preparation, Alignment, and Optical Properties of Soluble Poly(phenylacetylene)-Wrapped Carbon Nanotubes. *Macromolecules* **1999**, *32*, 2569–2576.
30. Yuan, W. Z.; Sun, J. Z.; Dong, Y. Q.; Haussler, M.; Yang, F.; Xu, H. P.; Qin, A. J.; Lam, J. W. Y.; Zheng, Q.; Tang, B. Z. Wrapping Carbon Nanotubes in Pyrene-Containing Poly(phenylacetylene) Chains: Solubility, Stability, Light Emission, and Surface Photovoltaic Properties. *Macromolecules* **2006**, *39*, 8011–8020.
31. Liu, W.; Yang, C. L.; Zhu, Y. T.; Wang, M. S. Interactions between Single-Walled Carbon Nanotubes and Polyethylene/Polypropylene/Polystyrene/Poly(phenylacetylene)/Poly(*p*-phenylenevinylene) Considering Repeat Unit Arrangements and Conformations: A Molecular Dynamics Simulation Study. *J. Phys. Chem. C* **2008**, *112*, 1803–1811.
32. Liu, J.; Rinzler, A. G.; Dai, H. J.; Hafner, J. H.; Bradley, R. K.; Boul, P. J.; Lu, A.; Iverson, T.; Shelimov, K.; Huffman, C. B.; *et al.* Fullerene Pipes. *Science* **1998**, *280*, 1253–1256.
33. Cohen, J. J. Apoptosis. *Immunol. Today* **1993**, *14*, 126–130.
34. Worle-Knirsch, J. M.; Pulskamp, K.; Krug, H. F. Oops They Did It Again! Carbon Nanotubes Hoax Scientists in Viability Assays. *Nano Lett.* **2006**, *6*, 1261–1268.
35. Pulskamp, K.; Diabat, S.; Krug, H. F. Carbon Nanotubes Show No Sign of Acute Toxicity but Induce Intracellular Reactive Oxygen Species in Dependence on Contaminants. *Toxicol. Lett.* **2007**, *168*, 58–74.
36. Petit, V.; Thiery, J. P. Focal Adhesions: Structure and Dynamics. *Biol. Cell* **2000**, *92*, 477–494.
37. Zachary, I.; Rozengurt, E. Focal Adhesion Kinase (p125FAK): A Point of Convergence in the Action of Neuropeptides, Integrins, and Oncogenes. *Cell* **1992**, *71*, 891–894.
38. Parsons, J. T.; Martin, K. H.; Slack, J. K.; Taylor, J. M.; Weed, S. A. Focal Adhesion Kinase: A Regulator of Focal Adhesion Dynamics and Cell Movement. *Oncogene* **2000**, *19*, 5606–5613.
39. Schaller, M. D.; Borgman, C. A.; Cobb, B. S.; Vines, R. R.; Reynolds, A. B.; Parsons, J. T. pp125FAK, a Structurally Distinctive Protein-Tyrosine Kinase Associated with Focal Adhesions. *Proc. Natl. Acad. Sci. U.S.A.* **1992**, *89*, 5192–5196.
40. Guan, J. L. Role of Focal Adhesion Kinase in Integrin Signaling. *Int. J. Biochem. Cell Biol.* **1997**, *29*, 1085–1096.
41. Tzoneva, R.; Faucheux, N.; Groth, T. Wettability of Substrata Controls Cell−Substrate and Cell−Cell Adhesions. *Biochim. Biophys. Acta* **2007**, *1770*, 1538–1547.